Resolution enhancement and improved data interpretation in electrostatic force microscopy

J. Colchero, A. Gil, and A. M. Baró
Departamento de Física de la Materia Condensada, Facultad de Ciencias, Universidad Autónoma de Madrid, E-28049 Madrid, Spain
(Received 24 February 2001; revised manuscript received 6 August 2001; published 28 November 2001)

The electrostatic interaction between a model probe and a sample in a scanning probe microscope is analyzed. A simple model for a real experimental setup is proposed and solved by means of an appropriate approximation. In addition, a quantitative definition for resolution is presented. We find that generally the total force between tip and sample is dominated by contributions which are not confined to a nanometer-sized region under the tip apex. From our analysis we conclude that such a confinement is only obtained either with specially designed probes or by using the force gradient as signal source. We show that reliable experimental data acquired by local Kelvin probe microscopy can only be obtained if these considerations are taken into account. Finally, we propose an experimental setup which optimizes resolution and gives the correct local surface potential in the case of Kelvin probe microscopy.

DOI: 10.1103/PhysRevB.64.245403 PACS number(s): 68.37.Ps, 07.50.−e, 07.79.Lh, 73.40.Cg

I. INTRODUCTION

The interaction of electric charges is without doubt the fundamental force that is best understood, and the one that has been verified experimentally with highest precision. Electrical forces govern most physical and chemical processes and, correspondingly, most technological applications are based on them. The modern computer industry patterns the electrical properties of materials on a (sub)micrometer scale to build operative devices. Also for the next step in miniaturization—namely, nanotechnology—electrostatic interaction is important. In the past decade the progress in this field has been remarkable. Part of this progress has been driven by the development of scanning probe microscopy,[1] which allows not only imaging and characterization of surfaces, but also their manipulation on a nanometer and even atomic scale. Among these techniques the scanning force microscope[2] (SFM) is probably the most versatile, since it allows different kinds of forces to be measured and in particular forces due to electric charges. If electrostatic forces are the main contribution to the total interaction in an SFM setup, one generally speaks of electrostatic force microscopy (ESFM). ESFM has been used to image charges,[3,4] dopant properties of semiconductors,[5] local surface potentials,[6,7] and even the adsorption of molecularly thin films of water on solid substrates.[8] In ultrahigh vacuum extremely high resolution of the local charge distribution and surface potential has been obtained.[9] We believe that this is not incidental, but related to the fact that in ultrahigh vacuum SFM experiments generally the frequency is used as an interaction signal.[10,11] As will be discussed in this work, this has important consequences for ESFM.

As on a larger scale, electrostatic interaction on a nanometer scale is the one with the highest strength, as well as the longest range compared to other relevant forces such as van der Waals or so-called ''chemical'' forces. A thorough discussion of the relative strengths and of the range of the different interactions relevant in SFM is given in Ref. 12. For the simplest cases of two infinite and parallel plates we find for the relation of van der Waals to electrostatic forces: $F_{vdW}/F_{el}=A/(6\pi\varepsilon_0 U^2 d)$. In this case the electrostatic interaction falls off faster than van der Waals interaction. At a distance of 2 nm the electrostatic interaction is stronger for voltages greater than about 0.5 V (a typical Hamaker constant $A\simeq 10^{-19}$ J is assumed). However, parallel plates are not a very physical model for an ESFM setup. Considering the more physical example of a cone we find that $F_{vdW}\sim 1/d$, while $F_{el}\sim\ln(h/d)$, where h is the height of the cone.[13] We note that to calculate the electrostatic force for an infinite object some cutoff length of the system is needed (here h); otherwise, the electrostatic interaction diverges due to the slow decay with distance. As will be discussed in this work, both its great strength and its large range lead to difficulties in understanding the details of this interaction as well as in interpretating data when electric forces are important in an SFM setup.

The purpose of the present paper is to present a realistic model to describe electrostatic interaction in a typical SFM setup. A definition of resolution in an ESFM is presented and applied to different experimental setups. As a result, appropriate operating conditions can be obtained which optimize resolution and greatly simplify data interpretation. In addition, we will show that when operating the ESFM in the so-called Kelvin probe mode, the classical measurement scheme may result in misinterpretation of experimental data. Finally we will propose an experimental setup based on the measurement of frequency shifts induced by electrostatic interaction which enhances resolution and yields correct values for the local surface potential. Although a similar idea has been applied already for the measurement of charges on surfaces[3] and is also used in ultrahigh vacuum,[9] we believe that right now its importance has not yet been recognized generally in ESFM. Moreover, to the best of our knowledge the scheme proposed here has not been applied to the local characterization of surface potentials. Without doubt the problems related to the classical detection scheme based on force measurements has slowed progress in a number of important nanoscale applications where ESFM is a fundamental tool.

II. MODELING THE PROBE-SAMPLE SYSTEM

One of the problems for modeling the electrostatic interaction in ESFM is its complexity. Therefore some simplified

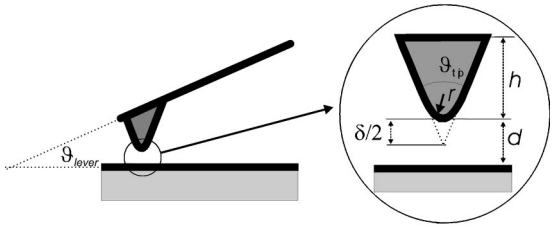

FIG. 1. Sketch of the model probe proposed for an ESFM setup. This probe is composed of three basic units: a cantilever of length l with tilting angle ϑ_{lever} with respect to the sample, a mesoscopic tip cone of height h, and (full) opening angle ϑ_{tip}, as well as a parabolic tip apex of radius r.

model system is used to describe the complex ESFM setup. In general the sample is assumed flat and some geometric entity is assumed as a ''tip.'' A simple charge,[14] a sphere,[3,15] or a cone[13] are the most used shapes. In some cases more sophisticated ''tips'' are proposed such as a spherical cap connected to a tip cone[16,17] or a sphere connected to a macroscopic cantilever.[18] Most studies assume a metallic tip and sample. The important case of dielectric samples is almost never treated due to its even greater complexity. Interesting approaches in this context are numerical calculations for thick dielectric samples[19] and a perturbative treatment[20] which can be applied for thin dielectric films on metallic samples.

In every setup, adequate modeling of the probe is fundamental. In our opinion the most appropriate assumption for such a probe in a real ESFM setup is a macroscopic cantilever, a mesoscopic tip cone, and a nanometer-sized tip apex (see Fig. 1). The latter is the relevant object for nanoscale experiments. However, all three components of the tip-lever system interact with the sample. Due to the slow decay of the interaction, the force induced by the mesoscopic tip cone and the cantilever will be in most cases greater than the force induced by the small tip apex, even though the latter is much closer to the sample. If the force induced by the tip apex is small compared to that induced by the lever and the tip cone, then ESFM is no longer a nanoscale measuring instrument or manipulation tool.

Another difficulty in modeling electrostatic interaction is that the distance dependence of the force cannot be calculated by adding the pairwise interaction of static charges at known positions. Such an approach makes the calculation of van der Waals forces comparatively easy: once the van der Waals ''charge density'' is specified through the Hamaker constant $A(\mathbf{x})$, the total interaction can be calculated by adding the pairwise interaction between different parts of the tip-sample system (see, for example, Refs. 21 and 22). In the case of electrostatic SFM, at least the tip is conducting;[23] therefore, as the tip-sample distance is varied, the charges on the tip can rearrange to minimize the total electrostatic energy of the system. The difference between the calculation of electrostatic forces and van der Waals forces is thus essentially related to the fact that electric charges can flow as the tip-sample distance is varied, while ''van der Waals charges'' are determined by the material of tip and sample and are fixed with respect to them.

Once the electric field distribution $\mathbf{E}(\mathbf{x})$ is known, the electrostatic interaction energy $W(d)$ between tip and sample can be calculated as[24]

$$W(d)=\int_{V(d)} dV \frac{\varepsilon_0}{2}\mathbf{E}(\mathbf{x})^2, \tag{1}$$

where $V(d)$ is the volume with nonvanishing electric field. As just discussed, when the tip-sample distance is varied, charges can flow and accordingly the field distribution $\mathbf{E}(\mathbf{x})$ changes. Therefore, to solve the integral (1), first the field distribution has to be determined. For an SFM setup where the tip and sample are metallic the electrostatic field is uniquely defined by the boundary condition that tip and sample be at well-defined potentials. In fact, if no additional charges are present between the conductors then for each tip-sample distance d the electric potential can be calculated from the boundary condition on the tip and sample and the differential equation $\Delta U(\mathbf{x};d)=0$ everywhere outside the conductors. The electric field is directly calculated as $\mathbf{E}(\mathbf{x};d)=\nabla_{\mathbf{x}}U(\mathbf{x};d)$ for each tip-sample distance d. If charges are present in the setup, then the calculation of the electrostatic force is less straightforward. In particular, the polarization of the charges between the metal surfaces has to be taken into account. A detailed analysis is found in Ref. 25.

In the present work we use a different approach to find the force between a metallic tip and a metallic sample by means of an approximation.[17,26] If the tip and sample are metallic, the field lines are aligned perpendicular to the conducting surfaces. To calculate the forces between tip and sample we will assume that the field lines can be approximated by segments of circles and that the electric potential decays linearly along these circular segments. In the present context, the sample S is flat and at the origin: $S=(x,y,0)$. The magnitude of the electric field on the sample is assumed to be simply $E_{approx}(x,y,d)=U/a(x,y,d)$, where U is the voltage between tip and sample and $a(x,y,d)$ the arc length of the circular segment coming from the tip and ending on a point (x,y) of the surface. This assumption is valid if the distance between the two conducting objects is not larger than their physical dimension.[27] Since ESFM is intrinsically a near-field technique, we will assume that this assumption is correct (see, however, the discussion in the Appendix). The electrostatic force between tip and sample is then

$$F(d)=\int_S dS \frac{\varepsilon_0}{2}\ E(x,y,d)^2 \simeq \frac{\varepsilon_0 U^2}{2}\int_S dS \frac{1}{a(x,y,d)^2}. \tag{2}$$

The first equation is exact and can be deduced by noting that the term $\varepsilon_0 E^2/2$ is the Maxwell stress—and thus a tension (unit:N/m^2)—acting on each point of the surface. Therefore the surface integral over this tension gives the total force acting on the surface due to the electrostatic interaction between tip and sample. The second term in relation (2) is obtained from the approximation discussed above, which we believe to be sufficiently good for typical experimental applications.

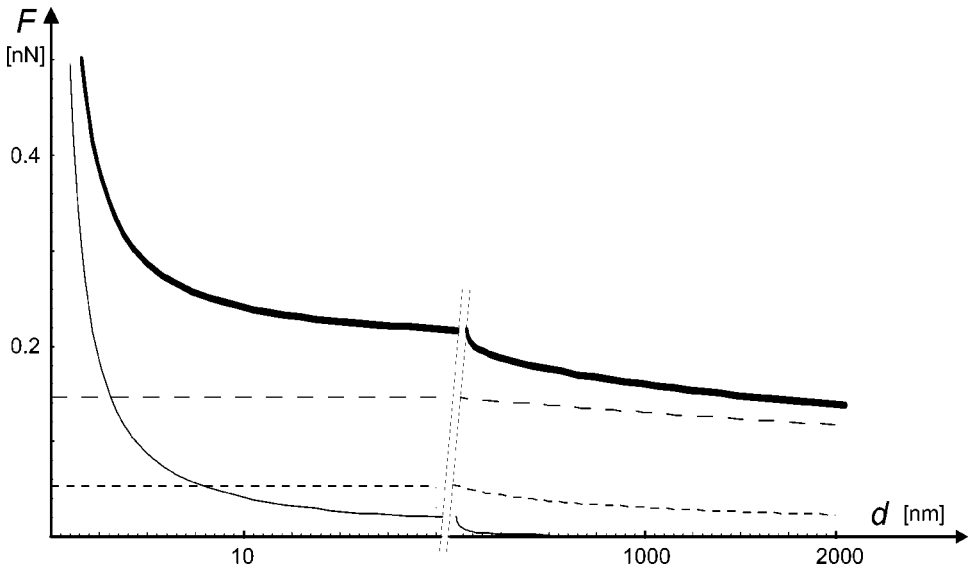

FIG. 2. Electrostatic force between a typical SFM probe and a flat metallic surface as a function of tip-sample distance. The thick line shows the total force; the thin solid line, short dotted line, and long dotted line correspond to the contributions from the tip apex, tip cone and cantilever respectively. The forces have been calculated for $U=1$ V and $l=100\ \mu$m, $w=20\ \mu$m, $\vartheta_{lever}=\pi/8$, $h=10\ \mu$m, $\vartheta_{tip}=\pi/8$, and $r=20$ nm.

To model electrostatic forces within a typical SFM setup we will assume that the tip-lever system has three elemental building blocks: a lever, a tip cone and a tip apex. The lever is characterized by its length l, its width w, and an angle ϑ_{lever} with respect to the sample surface. The tip is a truncated cone of height h and opening angle ϑ_{tip} which ends smoothly in a paraboloidal tip apex of radius r (see Fig. 1). For this geometry, the shape and length $a(x,y)$ of the circular segments connecting the probe and the sample can be calculated and relation (2) can be solved to obtain the following forces as a function of the distance d between the surface and the tip apex (see the Appendix):

$$F_{lever}(d) = f_{lev}\varepsilon_0 U^2 \frac{l\,w}{h^2}\,\frac{1}{(1+d/h)\{1+[d+2l\tan(\vartheta_{lever}/2)]/h\}}, \tag{3}$$

$$F_{cone}(d) = f_{cone}\,\varepsilon_0 U^2\left[\ln\left(\frac{d-\delta/2+h}{d+\delta/2}\right) - \sin(\vartheta_{tip}/2)\frac{h-\delta}{d-\delta/2+h}\,\frac{d-\delta/2}{d+\delta/2}\right], \tag{4}$$

$$F_{apex}(d) \simeq \frac{\pi\,\varepsilon_0 U^2}{1+f(\vartheta_{tip})(d/r)^2}\left(\frac{r+d/2}{r-2d}\right)^2\left(\frac{r-2d}{d[1+2\tan^2(\vartheta_{tip}/2)d/r]} + 2\ln\frac{4d}{2d+r+(r-2d)\cos(\vartheta_{tip})}\right), \tag{5}$$

where $f_{lev}=2\tan^2(\vartheta_{lever}/2)/\vartheta_{lever}^2$ and $f_{cone}=4\pi/(\pi-\vartheta_{tip})^2$ are geometrical factors, $f(\vartheta_{tip})=\ln[1/\sin(\vartheta_{tip}/2)]/\{[1-\sin(\vartheta_{tip}/2)][3+\sin(\vartheta_{tip}/2)]\}$, and $\delta=r/\tan^2(\vartheta_{tip}/2)$ is the height of the truncated part of the cone (see the Appendix). We recall that the force between two conducting bodies is related to the derivative of the capacitance: $F(d)=C'(d)U^2/2$, where $C(d)$ is the capacitance of the two conducting bodies. Therefore from Eqs. (3)–(5) the capacitances of the different components of the probe with respect to the sample can be obtained directly. The total capacitance of the ESFM setup is the sum of these individual capacitances, which means that the total capacitance of the system can be interpreted as individual capacitors in parallel.[28,29]

Figure 2 shows the total electrostatic force between a typical metallized model probe and a metallic flat sample. In addition, the individual contributions from the lever, cone, and tip apex are also shown. As can be seen from the graph, the contribution from the tip apex dominates only for distances smaller than about 3 nm. For larger distances the total interaction is dominated by F_{lever} or F_{cone}, and will therefore not yield any nanometer-scale resolution, since the sample is then probed by the mesoscopic tip cone and/or the macroscopic lever. In fact, in most experimental conditions the latter dominates and the resolution is of the order of the width of the cantilever—that is, several micrometers.

III. DEFINITION OF RESOLUTION

The reasoning just discussed gives a qualitative estimate of resolution. For a quantitative analysis of resolution first an appropriate definition is needed. In this context we recall that the integrand $\varepsilon_0 E^2(x,y,d)$ of Eq. (2) is the Maxwell tension which acts on each surface element of the sample. Therefore,

$$\delta^{force}(A,d) \equiv \frac{\int_A dS\,E^2(x,y,d)}{\int dS\,E^2(x,y,d)} = \frac{\varepsilon_0\int_A dS\,E^2(x,y,d)}{2\,F(d)}$$

is the relative contribution of an arbitrary area A to the total interaction. We now define resolution as the radius ρ of the

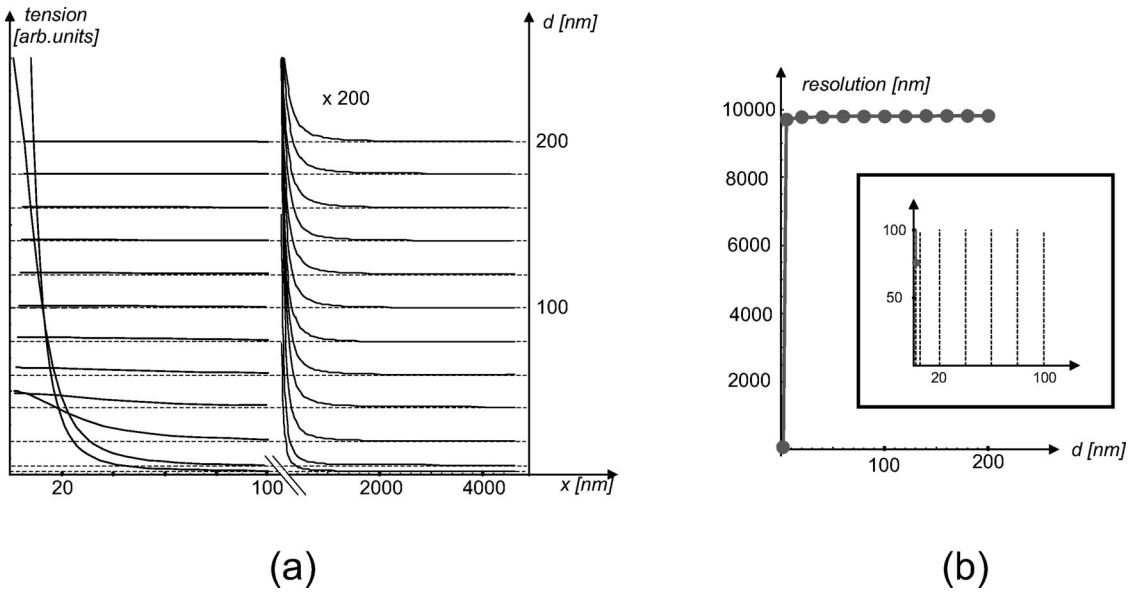

FIG. 3. As explained in the main text, the curve describing the lateral variation of the tension can be used to define an aperture function as well as a resolution. Graph (a) shows these (normalized) aperture functions for different tip-sample distances. Each curve has been offset with respect to the main origin of the graph by its corresponding tip-sample distance. The horizontal axis represents the distance to the symmetry axis of the system while the vertical axis is either the strength of the tension (in arbitrary units) or the tip-sample distance (offset for each tension curve). (b) The resolution $\mathrm{res}^{force}(d)$ has been calculated for the following tip-sample distances: $d=2,\ 5,\ 20,\ 40,\ 60,\ \ldots,180$, and 200 nm. The same parameters for the probe have been assumed as those applied for the calculation shown in Fig. 2: $U=1$ V, and $l=100\ \mu$m, $w=20\ \mu$m, $\vartheta_{lever}=\pi/8$, $h=10\ \mu$m, $\vartheta_{tip}=\pi/8$ and $r=20$ nm.

circle under the tip that contributes 1/2 to the total interaction:

$$\mathrm{res}^{force}(d) \equiv \text{radius } \rho \ \text{ such that } \delta^{force}(\pi\rho^2, d) = 1/2. \tag{6}$$

Figure 3 shows the (normalized) tensions as well as the resolution $\mathrm{res}^{force}(d)$ which have been calculated for different experimentally relevant tip-sample distances. We note that high resolution implies a low value for $\mathrm{res}^{force}(d)$. The same parameters for the probe have been used as those applied for the calculation of the forces shown in Fig. 2. Each curve representing the tension has been normalized with respect to the total force at that distance. In addition to the tensions, the lateral resolution has been calculated as defined by relation (6). As expected from the discussion based on the relative contribution of the forces induced by the different parts of the cantilever, the lateral resolution is of the order of micrometers for most tip-sample distances which are relevant $[2-200\ \mathrm{nm}=(0.1-10)r]$. Only for distances smaller than about 2 nm is the central peak of the tension induced by the interaction of the tip apex large enough to compensate for the rest of the tension induced by the long-range interaction of the tip cone and the cantilever. In fact, a more detailed analysis demonstrates that in the case shown the dominant interaction comes from the tension produced by the macroscopic cantilever rather than the tip cone (see also Fig. 2). This explains the low resolution and the fact that it is of the order of the width of the cantilever.

In conclusion, for typical cantilevers we find that the resolution is rather in the micrometer than in the nanometer range. Theoretically, nanometer resolution can be obtained for tip-sample distances smaller than about 2 nm. However, we believe that from an experimental point of view the measurement of electrostatic interaction at such small distances is an extremely difficult task. The required precise control of tip-sample distance without touching the surface is difficult in itself. In addition, for such small distances the electrostatic interaction induced by applying small voltages may induce snap-to contact and in air also condensation of water between tip and sample. Therefore, some other means of improving resolution has to be implemented.

IV. ENHANCEMENT OF RESOLUTION

A. Cantilever design

Relations (3)–(5) as well as the arguments just discussed guide the way to improving resolution: reduction of the ''long-range'' interaction area. This means that good electrostatic probes should have a small cantilever width, a small cone opening angle ϑ_{tip}, and a tip height of roughly the same value as the cantilever width: $w \approx h$. In addition, even though it may seem counterintuitive, a large tip radius will also increase resolution at intermediate distances, since it will increase the relative strength of F_{apex} with respect to the other two forces.[29] Of course the price for this increased resolution at an intermediate distance is a decreased one at very small distances. A second possibility to improve resolution is to use normal dielectric cantilevers patterned with a conductive layer on the tip side in an appropriate way: namely, a narrow conducting path covering the tip apex. Figure 4 shows the forces obtained for such a cantilever. For the parameters used the contribution of the lever to the total

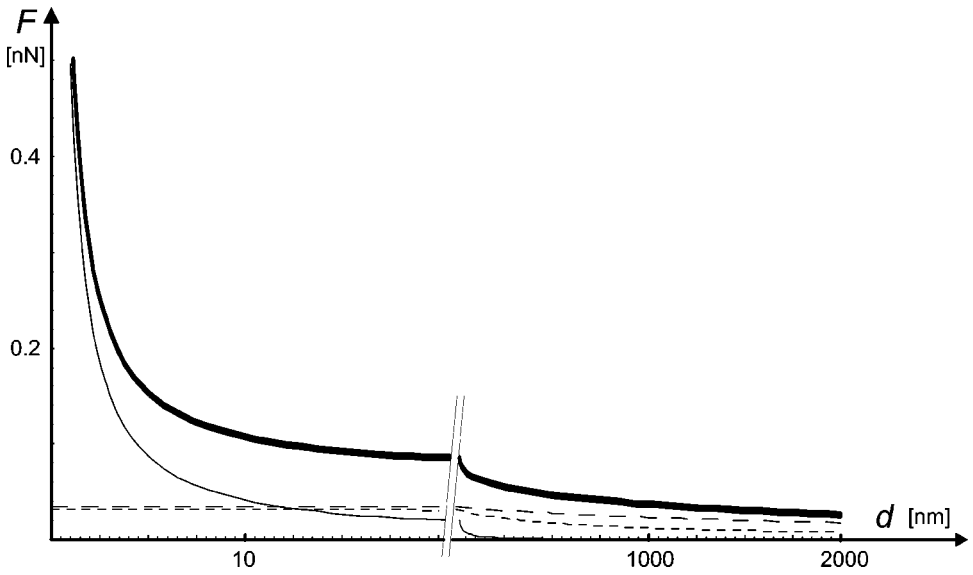

FIG. 4. Electrostatic force as a function of tip-sample distance for a cantilever which has been optimized for ESFM. As in Fig. 2, the thick line shows the total force. The thin solid line, short dotted line and long dotted line correspond to the contributions from the tip apex, tip cone, and cantilever, respectively. The parameters corresponding to the effective metallic probe interacting with the surface are $U=1$ V, and $l=100$ μm, $w=1$ μm, $\vartheta_{lever}=\pi/8$, $h=2.5$ μm, $\vartheta_{tip}=\pi/8$, and $r=20$ nm.

force has been reduced by a factor of 5 and that of the tip cone by a factor of 2 with respect to the cantilever modeled in Fig. 2.

B. Measurement of the force gradient

Another, even more drastic way of increasing the resolution of ESFM and to greatly simplify data interpretation is to change the signal source of the interaction. In fact, if the force gradient is measured instead of the force, the relative contribution of the tip apex to the total interaction is increased dramatically. This is shown in Fig. 5, where the total force gradient as well as the individual contributions of the cantilever, tip cone, and tip apex are computed for the same experimental system as that corresponding to Fig 2. If the force gradient is used to measure the interaction, relations (3)–(5) lead to the result that the contributions of the lever and tip cone are strongly reduced. The precise reduction factor is determined by the relative slope of the forces $F_{lever}(d)$ and $F_{cone}(d)$ with respect to $F_{apex}(d)$ at small distances ($d\simeq 0$). The reason for the strong reduction of the interaction induced by the lever and the tip is the low distance dependence of $F_{lever}(d)$ and $F_{cone}(d)$ on the range that is experimentally important. These large but constant force contributions are thus "differentiated away" when the force gradient is measured; therefore, only the term $F_{apex}(d)$ with the pole $1/d$ "survives."

Again, in addition to the qualitative discussion just presented, we have tried to find a quantitative definition of resolution. In analogy to the reasoning leading to relation (6), the integrand of

$$F'(h)=\frac{\varepsilon_0}{2}\int dS\,\frac{d}{dh}E^2(x,y,h) \tag{7}$$

can be used to define an aperture function. We note that in this case the integrand of relation (7) is not a tension as for the case of relation (2) but rather is in units of N/m^3. The relative contribution of an area A to the total force gradient is

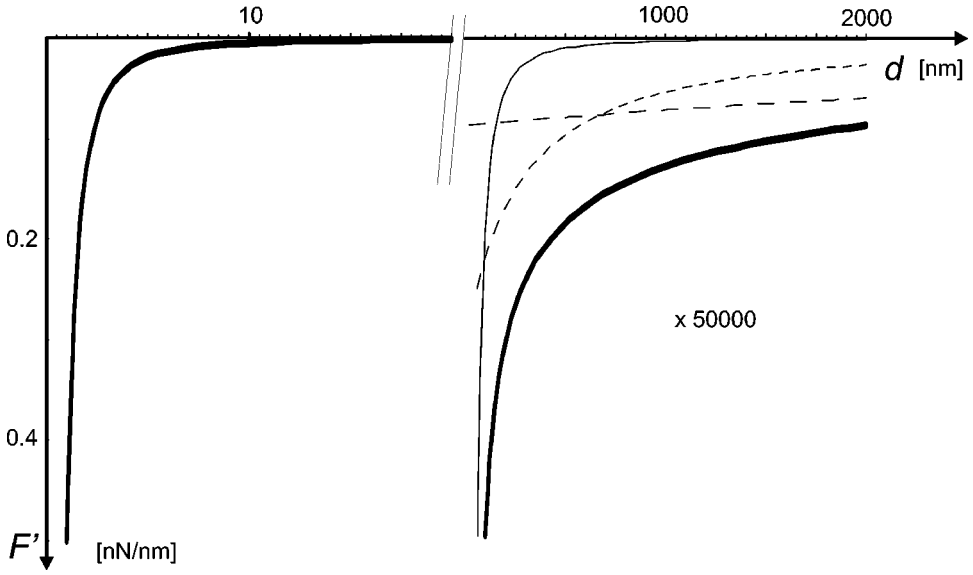

FIG. 5. Force gradient vs distance curve for the same probe as that used in Fig. 2 for the computation of the interaction force ($U=1$ V, and $l=100$ μm, $w=20$ μm, $\vartheta_{lever}=\pi/8$, $h=10$ μm, $\vartheta_{tip}=\pi/8$, and $r=20$ nm). For small tip-sample distances ($d\lesssim 50$ nm) the only relevant interaction is due to the tip apex (thin solid line).

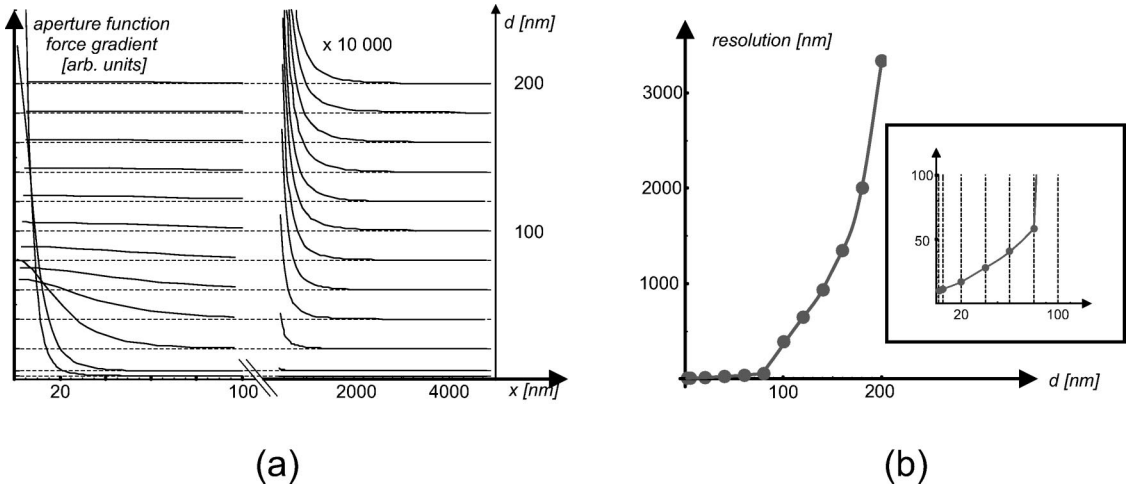

FIG. 6. (a) Aperture functions and (b) resolution $\mathrm{res}^{fg}(d)$ if the force gradient is used to measure the electrostatic interaction. These curves are analogous to those shown in Fig. 3. In (a) the horizontal axis represents the distance to the symmetry axis of the system, while the vertical axis is either the strength of the aperture function (in arbitrary units) or the tip-sample distance (offset for each aperture function). In (b) the horizontal axis represents tip-sample distance and the vertical axis the resolution. Note that the resolution is greatly enhanced as compared to the case shown in Fig. 3.

$$\delta^{fg}(A,h)\equiv\frac{\int_A dS\,\frac{d}{dh}E^2(x,y,h)}{\int dS\,\frac{d}{dh}E^2(x,y,h)}=\frac{\varepsilon_0\int_A dS\,\frac{d}{dh}E^2(x,y,h)}{2\,F'(h)},$$

and the resolution for the force gradient is defined as

$$\mathrm{res}^{fg}(d)\equiv\text{radius }\rho\text{ of the circle under the tip such that}$$
$$\delta^{fg}(\pi\rho^2,d)=1/2.$$

Figure 6 shows the lateral variation of the aperture function and the resolution $\mathrm{res}^{fg}(d)$ as a function of tip-sample distance. The same parameters for the probe have been used as those applied for the calculation shown in Figs. 2, 3, and 5. As can be seen by comparing Figs. 6 and 3 the resolution is greatly enhanced if the force gradient instead of the force is used to measure tip-sample interaction. For typical probe systems and typical tip-sample separations (10–20 nm) the resolution is increased by about 2 orders of magnitude.

An interesting feature which is observed in Figs. 3 and 6 is the sharp variation of resolution at some tip-sample distances. In Fig. 3 we find that at a distance of about 2 nm the resolution varies from about 10 μm to 100 nm. In Fig. 6 we find a transition of resolution at a tip-sample distance of about 80 nm. This is not an artifact of our calculation, but due to the fact that at these distances a different part of the probe becomes dominant. Indeed, as can be seen in Figs. 2 and 5, at distances larger than about 2 nm the force contribution from the cantilever starts to become greater than that of the tip apex (Fig. 2), while at distances larger than 100 nm the variation of the force gradient due to the tip cone is more important than that from the tip apex (Fig. 5). This is consistent with the sudden changes in resolution which we find at about the same distances in Figs. 3 and 6. Finally, we note that for all tip-sample distances the order of magnitude of the resolution is about the size of the geometric object which is dominant in the total interaction. We thus believe that we understand the details of how and why tip-sample interaction and resolution vary with tip-sample distance.

V. RESOLUTION AND KELVIN PROBE MICROSCOPY

In the discussion presented so far it may be argued that with regard to resolution the contributions due to F_{lever} and F_{cone} are not so critical since they only give large offset forces to the resolution carrying term F_{apex}. Therefore it could be argued that only the signal to noise ratio is lowered and not the resolution itself. However, in the so-called Kelvin probe microscopy (KPM), the contributions of the tip cone and the lever will induce severe errors in the measurement, as will now be discussed. We recall that the idea of KPM is to locally measure the surface potential.[6,7,28,30–32] KPM works by applying an adjustable bias voltage $U_{bias}(t)=U_{tip}+U_{ac}\sin(\omega_e t)$ between a conducting tip and the sample. Since the force is quadratic in the voltage, the measured force has components varying with the frequencies ω_e and $2\omega_e$ in addition to a static force. It is assumed generally that the total force can be written as

$$\begin{aligned}F_{tot}(d)&=\frac{1}{2}C'(d)[U_{bias}-U_{sample}]^2\\&=\frac{1}{2}C'(d)[\Delta U^2+U_{ac}^2/2\\&\quad+2\,\Delta U\;\;U_{ac}\,\sin(\omega_e t)-U_{ac}^2\cos(2\omega_e t)/2],\end{aligned}\tag{8}$$

where $\Delta U=U_{tip}-U_{sample}$, with U_{sample} the local voltage of the sample, is the (static) voltage difference between tip and sample and $C'(d)$ is the derivative of the capacitance of

the tip-sample system which depends on the geometric properties of the tip-sample system and can be determined from relations (3)–(5). In KPM a known voltage U_{tip} is applied to the tip so that the component $F^{\omega}=C'(d)\,\Delta U\,U_{ac}\sin(\omega_e t)$ vanishes. This seems to imply $U_{tip}=U_{sample}$ and thus that the local surface potential is measured. Relation (8) is, however, incorrect if the total force has contributions from different parts of the tip-lever system and if the surface potential varies locally—that is, if $U_{sample}=U_{sample}(x,y)$. Then, Eq. (2) has to be solved exactly. In the following, we will assume that tip and sample are conducting and that local variations of the surface potential are due to different metallic materials or to a very thin layer of dielectric material.[20,33] The approximation in relation (2) can then be generalized and the total force is computed as

$$F(d)=\frac{\varepsilon_0}{2}\int_S dS\,\frac{[U_{tip}-U_{sample}(x,y)+U_{ac}(t)]^2}{a(x,y)^2}. \quad (9)$$

The local surface potential as well as the applied alternating voltage therefore contribute to the total force in a nontrivial way and cannot be factored out. In particular we note that a surface potential distribution whose mean value vanishes ($\int dS\Delta U=0$) does necessarily mean that the electrical force also vanishes. To further illustrate the consequences of relation (9) in an experimentally realistic situation we will assume that an average global surface potential can be defined[34] and that the two relevant contributions to the total force are only due to the lever and the tip apex. Then the generalized relation (9) can be evaluated and yields for the component F^{ω}

$$F^{\omega}(d)=\{C'_{lever}(d)[U_{tip}-U_{global}] + C'_{apex}(d)[U_{tip}-U_{sample}(x,y)]\}U_{ac}\,\sin(\omega_{ac}t), \quad (10)$$

where C_{lever} and C_{apex} are the capacitances between lever and sample, and between tip apex and sample, respectively [see relations (3) and (5)]. This force component F^{ω} will vanish for[28,29]

$$U_{tip}=[C'_{lever}U_{global}+C'_{apex}U_{sample}(x,y)]/(C'_{lever}+C'_{apex}), \quad (11)$$

which is a weighted average of the global and the local surface potential, and not the true local potential. Even more discouraging, since $C'_{lever}(d)\gg C'_{apex}(d)$ for $d>r$, U_{tip} will be much closer to U_{global} than to $U_{sample}(x,y)$ for most tip-sample distances. As discussed previously, C_{lever} is almost constant for very small tip-sample distances while C_{apex} has a pole at $d=0$, and thus varies very considerably. Correspondingly, when tip-sample distance is very small the voltage needed to have $F^{\omega}=0$ is strongly distance dependent and thus meaningless.

A better measurement of local surface potential can be achieved again either by using a specially designed cantilever or by using the force gradient as interaction signal. In the latter case, a relation analogous to Eq. (10) is obtained for the force gradient component varying with $\sin(\omega_e t)$, but with the terms $C'_{lever}(d)$ and $C'_{apex}(d)$ substituted by $C''_{lever}(d)$ and $C''_{apex}(d)$:

$$F^{\omega\prime}(d)=\{C''_{lever}(d)[U_{tip}-U_{global}] + C''_{apex}(d)[U_{tip}-U_{sample}(x,y)]\}U_{ac}\,\sin(\omega_e t)$$
$$\approx C''_{apex}(d)[U_{tip}-U_{sample}(x,y)]U_{ac}\,\sin(\omega_e t).$$

As discussed in detail above, the contribution from the lever through $C''_{lever}(d)$ is then negligible with respect to $C''_{apex}(d)$. Therefore applying the Kelvin method we now obtain $U_{tip}\approx U_{sample}(x,y)$, which is what is wanted experimentally.

VI. RESOLUTION ENHANCEMENT: EXPERIMENTAL REALIZATION

The results on electrostatic interaction in a real SFM setup discussed so far lead to the conclusion that this interaction should generally be measured by relating it to the force gradient rather than to the force itself. The question is now how this can be realized experimentally. We propose to use a double lock-in detection scheme in which the cantilever is oscillated mechanically at its resonant frequency ω_m and the frequency variation of the system due to a time-varying electric voltage $U_{ac}\sin(\omega_e t)$ is measured. As is well known in SFM, a force gradient will induce a shift of the free resonant frequency according to[35]

$$\omega_m=\sqrt{\frac{c-\partial F(d)/\partial d}{m_{eff}}}\approx\omega_m\left(1-\frac{1}{2}\,\frac{\partial F(d)/\partial d}{c}\right),$$

where in the present context $F(d)$ is the electrostatic force between tip and sample just discussed, m_{eff} an effective mass, and c the force constant of the cantilever. This relation follows from modeling the tip-sample system as a harmonic oscillator and is only correct if the oscillation amplitude of the tip is small compared to the range over which the potential varies significantly.[36] If the frequencies ω_m and ω_e as well as the time constant τ of the lock-in detector associated with ω_m are adjusted appropriately (namely, $\omega_m>1/\tau>\omega_e$—for example, $\omega_m\approx 10/\tau\approx 100\,\omega_e$), then the frequency shift $\Delta\omega_m(t)$ of the mechanical oscillation can be determined very precisely with a second lock-in detector locked to ω_e. This second lock-in detector monitors the variation of the mechanical resonance frequency induced by the time-varying electrostatic field between tip and sample. The Kelvin method is implemented almost as in the usual way: an adjustable voltage U_{tip} as well as the additional harmonic voltage $U_{ac}\sin(\omega_e t)$ is applied to the tip. However, not the force, but the time-varying signal corresponding to the frequency shift $\Delta\omega_m(t)$ is monitored and analyzed with the help of the second lock-in detector. A feedback signal adjusts the tip voltage U_{tip} in such a way that the output related to the ω_e component of the frequency variation $\Delta\omega_m(t)$ vanishes.[37] Then the tip voltage U_{tip} is equal to the true local surface potential. We note that, in addition to the surface potential, also the local capacitance of the tip-sample

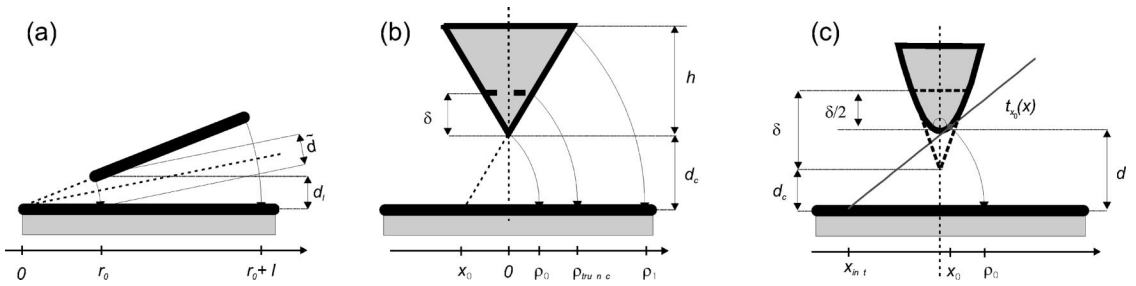

FIG. 7. Auxiliary sketches of (a) the lever-sample, (b) the cone-sample, and (c) the tip apex-sample system showing the parameters that are relevant for the calculation of the corresponding forces.

system can be measured with very high resolution. For this, the $2\omega_e$ component of the frequency variation $\Delta\omega_m(t)$ has to be determined with the second lock-in amplifier, in analogy to the classical KPM setup. This component is then proportional to $C''_{apex}U_{ac}^2$ and thus to the true local capacitance of the tip-apex system. The spatial resolution of the surface potential as well as for the local capacitance when measured as proposed along these lines is determined by the results shown in Fig. 6.

VII. CONCLUSION

In summary, we have presented a simple model for an SPM probe interacting with a flat sample surface. This model takes into account the contributions of the macroscopic cantilever, the mesoscopic tip cone as well as of the nanometric tip apex. Using an appropriate approximation, the force between this probe and the sample is calculated analytically as a function of tip-sample distance. We have found that only for very small tip-sample distances the total force is dominated by contributions from the tip apex. To improve resolution we propose to use either specially shaped cantilevers or the force gradient as signal source for the interaction. In addition, our analysis has shown that the common way of acquiring data in KPM leads to severe errors when the local surface potential is measured. Finally, we have proposed an SFM setup to implement quantitative local ESFM and in particular true local KPM, which is based on the measurement of the force gradient rather than of the force. We believe that the results discussed in the present work will lead to both a significant increase in electrostatic resolution as well as a quantitative determination of electrical properties on a nanometer scale.

ACKNOWLEDGMENTS

The authors thank J.J. Saenz, S. Gómez-Moñivas, R. Reitenberger, L.S. Froufe-Pérez, P.J. de Pablo, and J. Gómez for interesting discussions and valuable suggestions. We acknowledge support from Ministerio de Educación y Cultura through a CYCIT Project No. PB95-0169 and a contract to J. Colchero. A. G. acknowledges support from the FGUAM through the project ''Nanodigital.''

APPENDIX

In what follows we will explain how Eqs. (3)–(5) have been obtained for the different individual components of the model probe system—namely, the macroscopic lever, the (truncated) tip cone, and the parabolic tip apex (see Figs. 1 and 7). As discussed in the main text, the idea of the approximation used in the present work is to connect each point between the model probe with circular segments which enter perpendicular into tip and sample (both are assumed metallic). The main difficulty with this approach is to find a relation for the arc length $a(x,y)$ which can be integrated analytically. Each part of the model system will be treated individually.

1. Lever

The lever is assumed rectangular of width w and length l and tilted ϑ_{lever} with respect to the sample [see Fig. 7(a)]. Lines passing through the lever and the sample join at a point which is assumed to be the origin of the coordinate system. We note that the system is symmetric with respect to a line passing through the origin with an angle $\vartheta_{lever}/2$. Due to this symmetry, in the present context it is more natural to measure distances perpendicular to the symmetry line of the system (termed $\tilde{d}$). From Fig. 7(a) one finds $\tilde{d} = d_l \cos(\vartheta_{lever}/2)$ for the closest distance between lever and sample. The radius of the arc connecting this closest end of the lever with the sample is given by $r_0 = \tilde{d}/[2\sin(\vartheta_{lever}/2)] = d_l \cot(\vartheta_{lever}/2)/2$ and the corresponding arc length is $a_0 = r_0\vartheta_{lever}$. For an arbitrary point of the sample we find an arc length

$$a(x,y) = x\vartheta_{lever} \quad \text{with} \quad r_0 \leqslant x \leqslant r_0 + l \quad \text{and} \quad -w/2 \leqslant y \leqslant w/2.$$

The total force is thus given by

$$F^{lever}(d_l) = \frac{1}{2}\varepsilon_0 U^2 \int_{-w/2}^{+w/2}\int_{r_0}^{r_0+l} dxdy \frac{1}{x^2\vartheta_{lever}^2}$$

$$= \frac{2\,\tan^2(\vartheta_{lever}/2)}{\vartheta_{lever}^2}\varepsilon_0 U^2$$

$$\times \frac{l\,w}{d_l^2}\frac{1}{1+2l\tan(\vartheta_{lever}/2)/d_l}$$

$$\simeq \frac{1}{2}\varepsilon_0 U^2 \frac{wl}{d_l^2}\frac{1}{1+l\,\vartheta_{lever}/d_l}.$$

The approximation is valid for small tilting angles. We note that in the limit $\vartheta_{lever} \to 0$ the relation for the parallel capacitor is obtained correctly.

2. Cone

The tip is assumed a circular cone of height h and (full) opening angle ϑ_{tip} [see Figs. 1 and 7(b)]. The origin is on the symmetry axis of the system. The radius of the arc leaving the tip end is $r_0 = d_c/\cos(\vartheta_{tip}/2)$ and the corresponding center of the arc is $(x_0,0)$, with $x_0 = -d_c \tan(\vartheta_{tip}/2)$. The position on the surface where this arc ends is $\rho_0 = x_0 + r_0 = d_c[1-\sin(\vartheta_{tip}/2)]/\cos(\vartheta_{tip}/2)$. Similarly, the position on the surface where the arc from the top of the cone ends is $\rho_1 = d_c[1-\sin(\vartheta_{tip}/2)+h/d_c]/\cos(\vartheta_{tip}/2)$. Since the radius of the arc increases linearly with distance on the sample surface, we find for this radius r_{arc} and for the arc length a

$$r_{arc}(\rho) = r_0 + (\rho - \rho_0) \quad \text{and} \quad a(\rho) = \left(\frac{\pi}{2} - \frac{\vartheta_{tip}}{2}\right) r(\rho).$$

For the force acting on the cone we obtain

$$\begin{aligned}
\tilde{F}^{cone}(d_c) &= \frac{1}{2}\varepsilon_0 U^2 2\pi \int_{\rho_0}^{\rho_1} \rho d\rho \frac{1}{a(\rho)^2} \\
&= \frac{4\pi}{(\pi-\vartheta_{tip})^2}\varepsilon_0 U^2 \left[\frac{(\rho_0 - r_0)(\rho_1-\rho_0)}{r_0(\rho_1-\rho_0+r_0)} \right. \\
&\quad \left. + \ln\left(1+\frac{\rho_1-\rho_0}{r_0}\right)\right] \\
&= \frac{4\pi}{(\pi-\vartheta_{tip})^2}\varepsilon_0 U^2 \left(\ln\frac{d_c+h}{d_c} - \sin(\vartheta_{tip}/2)\frac{h}{h+d_c}\right) \\
&\simeq \frac{4\pi}{(\pi-\vartheta_{tip})^2}\varepsilon_0 U^2 \left(\ln\frac{h}{d_c} - \sin(\vartheta_{tip}/2)\right),
\end{aligned}$$

where the expressions for r_0, ρ_0, and ρ_1 discussed above have been used. The approximation is valid for $d_c \ll h$. Finally, if the tip is not a sharp cone but a truncated one where a height δ of the tip end has been removed, then the lower limit of the integral is not ρ_0, but $\rho_{trunc} = d_c[1-\sin(\vartheta_{tip}/2) + \delta/d_c]/\cos(\vartheta_{tip}/2)$, and the corresponding force is

$$\begin{aligned}
&F^{cone}(d) \\
&= \frac{1}{2}\varepsilon_0 U^2 2\pi \int_{\rho_{trunc}}^{\rho_1} \rho d\rho \frac{1}{a(\rho)^2} \\
&= \frac{4\pi}{(\pi-\vartheta_{tip})^2}\varepsilon_0 U^2 \left(\ln\frac{d_c+h}{d_c+\delta} \right. \\
&\quad \left. - \sin(\vartheta_{tip}/2)\frac{h-\delta}{d_c+h}\frac{d_c}{d_c+\delta}\right) \\
&\simeq \frac{4\pi}{(\pi-\vartheta_{tip})^2}\varepsilon_0 U^2 \left(\ln\frac{h}{d_c+\delta} - \sin(\vartheta_{tip}/2)\frac{1}{1+\delta/d_c}\right).
\end{aligned}$$

Again, the approximation is valid for $d_c \ll h$. We note that tip-sample distance is now $d_c+\delta$ and not simply d_c as for a sharp cone. In particular, the force does not diverge for $d_c = 0$, but for $d_c = -\delta$. Instead, for $d_c \to 0$ we find a constant force $F^{cone} = 4\pi\varepsilon_0 U^2 \ln(h/\delta)/(\pi-\vartheta_{tip})^2$. This behavior is reasonable since the truncated cone is touching the surface only for $d_c = -\delta$.

3. Parabolic apex

The tip apex is assumed to be a parabolic cap which joins smoothly with the truncated cone [see Fig. 7(c)]. Thus the slope of the line defining the cone and the slope of the parabolic cap have to be equal. From this, the equation describing the parabolic cap $c(x)$ follows as

$$c(x) = \frac{1}{2r}x^2 + d \quad \text{with} \quad |x| < \frac{r}{\tan(\vartheta_{tip}/2)}.$$

At each point x_0 of the tip apex its tangent has a slope x_0/r and the equation describing this tangent is

$$t_{x_0}(x) = \left(\frac{x_0}{r}\right)(x-x_0) + c(x_0).$$

The corresponding intersection point with the sample is found to be $x_{int}(x_0) = x_0/2 - d\,r/x_0$. With this point the radius of the arc $r_{arc}(x_0)$ as well as the arc $a(x_0)$ itself is

$$r_{arc}^2(x_0) = (x_0 - x_{int}(x_0))^2 + c(x_o)^2$$

and

$$a^2(x_0) = \left(\frac{x_0}{r}\right)^2 r_{arc}^2(x_0).$$

This relation expresses the arc length as a function of x, that is, the projection of the parabola onto the x axis, and not as a function of the position ρ where the arc leaving the apex hits the sample. This position is found to be $\rho(x_0) = x_{int}(x_0) + r_{arc}(x_0)$. Unfortunately we have not been able to find a simple relation for the arc length r_{arc} as a function of ρ to solve the correct integral (2) analytically. Therefore we have approximated the correct integral by assuming a linear relation between ρ and x. We then have

$$\begin{aligned}
\tilde{F}^{apex}(d) &= \frac{1}{2}\varepsilon_0 U^2 2\pi \int_0^{\rho_{\max}} \rho d\rho \frac{1}{a(\rho)^2} \\
&= \pi\varepsilon_0 U^2 \int_0^{x(\rho_{\max})} d\rho \frac{\rho(x)}{a(\rho(x))^2}\frac{d\rho}{dx}dx \\
&\simeq \pi\varepsilon_0 U^2 (1+d/2r)^2 \int_0^{x(\rho_{\max})} dx \frac{x}{a(x)^2} \\
&= \pi\varepsilon_0 U^2 \left(\frac{r+d/2}{r-2d}\right)^2 \left(\frac{1}{d}\frac{r-2d}{1+2d\tan^2(\vartheta_{tip}/2)/r} \right. \\
&\quad \left. + 2\ln\frac{4d}{2d+r+(r-2d)\cos(\vartheta_{tip})}\right) \\
&\simeq \pi\varepsilon_0 U^2 \frac{r}{d}, \qquad \text{(A1)}
\end{aligned}$$

where the relation $\rho(x) \simeq x(1+d/2r)$ has been used and the approximation is valid again for very short distances, in this

case for $d \ll r$. The asymptotic limit of $\tilde{F}^{apex}(d)$ is thus the same as the limit which is obtained from the exact solution of a conducting sphere over a conducting infinite surface.[38] We note that for $d \to r/2$ relation (A1) does not diverge, instead we find $\tilde{F}^{apex}(r/2) = \pi \varepsilon_0 U^2 (5/4)^2 \cos^2(\vartheta_{tip}/2) \times [3 - \cos(\vartheta_{tip})]/2$ and that $\tilde{F}^{apex}(\infty) = \pi \varepsilon_0 U^2 \ln[1/\sin(\vartheta_{tip}/2)]/4$. The latter limit is in contradiction to the limit which is obtained from the exact relation. This behavior is related to the fact that, as discussed in Sec. II, Eq. (2) is only valid in the near-field regime. In case of the tip apex this implies $r \lesssim d$. However, in an ESFM setup ranges larger than this are also of experimental relevance. Therefore we propose the following empirical relation for the electrostatic force on the tip apex:

$$F^{apex}(d) \simeq \frac{\pi \varepsilon_0 U^2}{1 + f(\vartheta_{tip})(d/r)^2} \left(\frac{r + d/2}{r - 2d} \right)^2 \times \left(\frac{r - 2d}{d[1 + 2\tan^2(\vartheta_{tip}/2) d/r]} + 2 \ln \frac{4d}{2d + r + (r - 2d)\cos(\vartheta_{tip})} \right), \quad \text{(A2)}$$

with $f(\vartheta_{tip}) = \ln[1/\sin(\vartheta_{tip}/2)]/\{[1 - \sin(\vartheta_{tip}/2)][3 + \sin(\vartheta_{tip}/2)]\}$. The additional factor $1/[1 + f(\vartheta_{tip})(d/r)^2]$ in $F^{apex}(d)$ as compared to $\tilde{F}^{apex}(d)$ does not vary the short-range behavior and gives the correct limit for $d \gg r$.

4. Composite system: Lever-cone-parabolic cap

The forces between the individual components of the model probe have been determined as a function of distance. However, when assembling these individual components into the model probe as shown in Fig. 1 it is important to redefine the distances correctly for each component. For the model probe we define tip-sample distance d as the separation between the paraboloidal apex and the sample; thus, $d = d_{apex}$, where d_{apex} is the separation discussed in the previous section.

The height of the truncated part of the cone is $\delta = r/\tan^2(\vartheta_{tip}/2)$. However, in the case of the conical tip the distance d_c was calculated from the end of a sharp conical tip, which is not the distance d. From elementary geometry [see Fig. 7(c)] we find

$$d_c + \delta = d + \frac{1}{2r} \left(\frac{r}{\tan(\vartheta_{tip}/2)} \right)^2 = d + \frac{\delta}{2}.$$

Finally the distance between the surface and the lever is simply $d_l = d_c + h \simeq d + h$, with h tip height. The forces on the cone and the lever in our model system are therefore

$$F^{lever}(d) = \frac{2\tan^2(\vartheta_{lever}/2)}{\vartheta_{lever}^2} \varepsilon_0 U^2 \times \frac{l\,w}{(d+h)^2} \frac{1}{1 + 2l\tan(\vartheta_{lever}/2)/(d+h)} \simeq \frac{2\tan^2(\vartheta_{lever}/2)}{\vartheta_{lever}^2} \varepsilon_0 U^2 \times \frac{w}{h} \frac{1}{h + 2l\tan(\vartheta_{lever}/2)},$$

$$F^{cone}(d) = \frac{4\pi}{(\pi - \vartheta_{tip})^2} \varepsilon_0 U^2 \left[\ln\left(\frac{d - \delta/2 + h}{d + \delta/2} \right) - \sin(\vartheta_{tip}/2) \frac{h - \delta}{d - \delta/2 + h} \frac{d - \delta/2}{d + \delta/2} \right] \simeq \frac{4\pi}{(\pi - \vartheta_{tip})^2} \varepsilon_0 U^2 \left[\ln\left(\frac{2h}{\delta} \right) + \sin(\vartheta_{tip}/2) \right].$$

Again, the approximations are valid for very small tip-sample distances ($d \ll r$ and $d \ll h$). The force on the apex is given by relation (A2).

[1] G. Binnig, H. Rohrer, Ch. Gerber, and E. Weibel, Phys. Rev. Lett. **49**, 57 (1982).

[2] G. Binnig, C.F. Quate, and Ch. Gerber, Phys. Rev. Lett. **56**, 930 (1986).

[3] B.D. Terris, J.E. Stern, D. Rugar, and H.J. Mamin, Phys. Rev. Lett. **63**, 2669 (1989).

[4] Ch. Schoenenberger and S.F. Alvarado, Phys. Rev. Lett. **65**, 3162 (1990).

[5] D.W. Abraham, C. Williams, J. Slinkman, and H.K. Wichramasinghe, J. Vac. Sci. Technol. B **9**, 703 (1991).

[6] D.W. Abraham and H.K. Wichramasinghe, J. Vac. Sci. Technol. B **9**, 1559 (1991).

[7] J.M.R. Weaver and D.W. Abraham, J. Vac. Sci. Technol. B **9**, 1559 (1991).

[8] J. Hu, X.D. Xiao, D.F. Ogletree, and M. Salmerón, Science **268**, 267 (1995).

[9] S. Kitamura and M. Iwatsuki, Appl. Phys. Lett. **72**, 3154 (1998).

[10] L. Howald, R. Lüthi, E. Meyer, P. Güthner and H.-J. Güntherodt, Z. Phys. B: Condens. Matter **93**, 267 (1994).

[11] F.J. Giessibl, Science **267**, 1451 (1995).

[12] M. Guggisberg, M. Bammerlin, Ch. Loppacher, O. Pfeiffer, A. Abdurixit, V. Barwich, R. Bennewitz, A. Baratoff, E. Meyer, and H.-J. Güntherodt, Phys. Rev. B **61**, 11151 (2000).

[13] H.W. Hao, A.M. Baró, and J.J. Sáenz, J. Vac. Sci. Technol. **9**, 1323 (1991).

[14] J. Hu, X.D. Xiao, and M. Salmerón, Appl. Phys. Lett. **67**, 476 (1995).

[15] P. Franz, N. Agrait, and M. Salmerón, Langmuir **12**, 3289 (1996).

[16] S. Beladi, P. Girard, and G. Leveque, J. Appl. Phys. **81**, 1023 (1997).
[17] S. Hudlet, M. Saint Jean, C. Guthmann, and J. Berger, Eur. Phys. J. B **2**, 5 (1998).
[18] L. Xu and M. Salmeron, *Nano-Surface Chemistry*, edited by M. Rosoff (Dekker, New York, in Press).
[19] S. Gómez-Moñivas, L.S. Froufe-Pérez, A.J. Caamaño, and J.J. Sáenz, Appl. Phys. Lett. (in press).
[20] S. Gómez-Moñivas, J.J. Sáenz, R. Carminatti, and J.J. Greffet, Appl. Phys. Lett. **76**, 2955 (2000).
[21] J. N. Israelachvili, *Molecular and Intermolecular Forces* (Academic Press, San Diego, 1992).
[22] C. Argento and R.H. French, J. Appl. Phys. **80**, 6081 (1996).
[23] Otherwise it is very difficult to define the tip electrostatically: how does one attach charges to the tip apex in a controlled way?
[24] J. D. Jackson, *Classical Electrodynamics*, 3rd ed. (John Wiley & Sons, New York, 1998).
[25] L.N. Kantorovich, A.I. Livshits, and A.M. Stoneham, J. Phys.: Condens. Matter **12**, 795 (2000).
[26] In addition, we assume no charges between tip and sample. If charges are present, see the discussion in Ref. 25.
[27] For very large distances, the field from the tip is similar to that produced by a point charge in front of a conducting wall. One then finds by the ''image method'' that $E(x,y,d)$ is proportional to $U_0/(x^2+y^2+d^2)$.
[28] T. Hochwitz, A.K. Henning, C. Levey, C. Daghlian, and J. Slinkman, J. Vac. Sci. Technol. B **14**, 457 (1996).
[29] H.O. Jacobs, P. Leuchtmann, O.J. Homan, and A. Stemmer, J. Appl. Phys. **84**, 1168 (1998).
[30] M. Nonnenmacher, M.P. O'Boyle and H.K. Wichramasinghe, Appl. Phys. Lett. **58**, 2921 (1991).
[31] H.O. Jacobs, H.F. Knapp, S. Müller, and A. Stemmer, Ultramicroscopy **69**, 39 (1997).
[32] J. Lü, E. Delamarche, L. Eng, R. Bennewitz, E. Meyer, and H.-J. Güntherodt, Langmuir **15**, 8184 (1999).
[33] For the discussion presented here to be valid it is important that the field lines stand perpendicular to the sample so that the approximation used is valid.
[34] A global mean voltage under the cantilever is defined through $\overline{U}=\sqrt{\int U(x,y)^2 dS}/A$.
[35] U. Dürig, O. Züger, and A. Stalder, J. Appl. Phys. **72**, 1778 (1992).
[36] To be more precise, the effective force constant $c_{eff}=c-\partial F(d)/\partial d$ of the system should not vary significantly over the range of cantilever oscillation. This implies that $|F''(d_0)|a \ll c_{lever}$, where a is the oscillation amplitude, $F''(d_0)$ the second derivative of the force at the mean equilibrium position d_0, and c_{lever} the force constant of the cantilever.
[37] We note that, in analogy to the electrostatic force between tip and sample, also the signal corresponding to the frequency shift will have three components: a dc component as well as a component varying with ω_e (more precisely: $\Delta\omega_m^1(t)=\Delta\omega_m^1 \sin[\omega_e t]$) and another one varying with $2\omega_e$ (more precisely: $\Delta\omega_m^2(t)=\Delta\omega_m^2 \sin[2\omega_e t]$). The idea is to adjust U_{tip} so that $\langle\Delta\omega_m^1(t)\rangle=0$.
[38] The exact solution of a (full) sphere over a conduction surface is $F(d)=C'(d)U^2/2$, where the capacitance $C(d)$ is determined through an an infinite sum: $C(d)=4\pi\varepsilon_0 r \sinh\xi(d)\Sigma_j \cosh j\,\xi(d)$ and $\xi(d)=\cosh^{-1}(1+d/r)$. See also W.R. Smythe, *Static and Dynamic Electricity* (McGraw-Hill, New York, 1939), p. 131.